Nuclear Magnetic Resonance of H^1 and Nb^{93} in the Niobium-Hydrogen System*

DAVID ZAMIR AND R. M. COTTS†
Laboratory of Atomic and Solid State Physics, Cornell University, Ithaca, New York
(Received 2 December 1963)

The nuclear magnetic resonance of H and Nb^{93} have been observed in the NbH_x system as a function of hydrogen concentration and temperature. It is shown that line narrowing of the steady-state absorption resonance is limited at high temperatures by inhomogeneous broadening due to a distribution of fields caused by bulk paramagnetism of the samples. A sharp, though not discontinuous, change of hydrogen diffusion is observed at temperatures that range from 60 to 100°C and that depends on hydrogen concentration. Niobium resonance linewidth and intensity changes indicate that sharp change in proton diffusion is associated with the phase transition to the high-temperature cubic phase of the hydrides. The activation energy of $NbH_{0.7}$ is $E_a=5$ kcal/mole in the low-temperature (orthorhombic) phase and $E_a=3.7$ kcal/mole in the high-temperature (cubic) phase. The niobium resonance is observable at all hydrogen concentrations. As the hydrogen concentration increases, the Nb Knight shift decreases. The fractional change in shift is $\Delta K/K=-9\%$ at $NbH_{0.7}$.

I. INTRODUCTION

NIOBIUM metal reacts exothermically with hydrogen and will form hydrides, NbH_x, with $x\leq 1$. X-ray diffraction experiments[1–5] indicate that up to a composition of $NbH_{0.1}$, the hydrogen enters in solution in the slightly expanded body-centered cubic lattice of niobium. Above a composition of $NbH_{0.1}$, a hydrogen-rich phase is found which is a slightly distorted bcc lattice and has been reported[1,4,5] to be orthorhombic. The x-ray experiments[3,5] also give evidence for a phase transition from the orthorhombic to a bcc phase at temperatures above about 100°C, which depend on x in NbH_x.

The present study was initiated to investigate diffusion of hydrogen in the Nb-H system and to determine the dependence of the Nb Knight shift[6] upon hydrogen concentration.

The nuclear magnetic resonance (NMR) spin dephasing time T_2 and the thermal relaxation time T_1 are very sensitive to translational diffusion of atoms in the lattice. Activation energies for self-diffusion of the hydrogen ion in the transition metal hydrides are not large, and high rates of diffusion occur below a few hundred degrees centigrade and in some cases at temperatures well below room temperature. The immediate atomic environment around the metal ion often has low symmetry due to random hydrogen ion occupation of interstitial sites in the metal lattice. Even in ordered structures, there can be a high concentration of defects (1–3%) at moderate temperatures.[7] If the nucleus of the metal ion has an electric quadrupole moment, a distribution of nuclear environments having symmetry lower than tetrahedral or cubic can produce a distribution of electric field gradients over nuclear sites in the crystal. At low temperatures, with the hydrogen ions fixed in position, the distribution of nuclear electric quadrupole interactions can broaden the resonance line beyond detectability.

It has been shown[8] that at high temperatures the quadrupolar broadening is motionally narrowed by rapid hydrogen diffusion and the metal ion NMR becomes observable. This situation obtains in NbH_x.

Because of the broadening of NMR linewidths as observed by steady-state techniques due to bulk magnetic susceptibility,[9] there is a lower limit on the observed widths of diffusion-narrowed proton resonance lines. This field-dependent inhomogeneous broadening could account for the field-dependent width observed in solid sodium.[10] Because the internal field within each metal particle will in general not be uniform, one can expect that at very high temperatures the effects of diffusion in a magnetic field gradient[11] will be observed.

II. APPARATUS AND MEASUREMENTS

Steady-state NMR absorption measurements were made by using a Varian wide-line rf unit and probes (nuclear induction). Pulsed free induction decay and spin-echo observations were made at 6.95 and at 11.65 Mc/sec. Only the proton resonance was observed with the pulse apparatus.

For most measurements, temperature control was maintained by using an L-shaped Dewar insert through which dry nitrogen gas was passed at an adjustable rate. Cooled nitrogen was obtained by controlled boiling

* This work was supported by the National Science Foundation and the Advanced Research Projects Agency.
† 1963–1964 address: Metallurgy Division, National Bureau of Standards, Washington, D. C.
[1] G. Brauer and R. Hermann, Z. Anorg. Allgem. Chem. **11**, 274 (1953).
[2] W. Trzebiatowski and B. Stalinski, Bull. Acad. Polon. Sci. Ser. Sci. Tech. III **7**, 317 (1953).
[3] W. Albrecht, W. Goode, and M. Mallett, Report No. BMI-1332, April 1959, Battelle Memorial Institute, Columbus, Ohio (unpublished).
[4] H. W. Paxton, J. M. Sheehan, and W. J. Babyak, Trans. Met. Soc. AIME **215**, 725 (1959).
[5] C. Wainwright, Bull. Instr. Metals **4**, 68 (1958).
[6] W. D. Knight, Solid State Phys. **2**, 93 (1956); T. J. Rowland, Progr. Mater. Sci. **9**, 1 (1961).
[7] G. Libowitz, Bull. Am. Phys. Soc. **7**, 438 (1962).
[8] D. S. Schreiber and R. M. Cotts, Phys. Rev. **131**, 1118 (1963).
[9] L. E. Drain, Proc. Phys. Soc. (London) **80**, 1380 (1962).
[10] F. J. Leech, L. C. Brown, and J. R. Gaines, Phys. Rev. Letters **11**, 121 (1963).
[11] H. Y. Carr and E. M. Purcell, Phys. Rev. **94**, 630 (1954).

of liquid nitrogen. For high temperature, the current in a heater in the Dewar was adjusted manually for steady-state temperature at the sample. Sample temperatures were monitored with a copper-constantan thermocouple mounted just above the sample. The temperature measurements are accurate to $\pm 1°C$.

Samples of NbH_x were prepared with a known amount of hydrogen determined by the system volume and measured pressure. Niobium metal powder (99.7% pure) was heated to 300°C and then the hydrogen was gradually allowed to combine with the metal. After hydriding, samples were cooled to room temperature, the sample vial was filled with argon gas and sealed off. Relative hydrogen concentration was checked by numerical integration of NMR absorption signals. Sample concentrations are accurate to three percent.

III. PROTON MAGNETIC RESONANCE

1. Rigid Lattice Second Moments

For powder samples used, the second moment $\langle \Delta H^2 \rangle$ of the proton magnetic resonance is given by[12]

$$\langle \Delta H^2 \rangle = \tfrac{3}{5}\gamma_I^2\hbar^2 I(I+1)\sum_i (r_i^{-6}) + (4/15)\gamma_S^2\hbar^2 S(S+1)\sum_i (r_j)^{-6}, \quad (1)$$

where γ_I and γ_S are the gyromagnetic ratios of the protons and niobium spins and I and S are the proton and niobium spin quantum numbers. The large spin of niobium, $S=\frac{9}{2}$, offsets its smaller γ_S with the result that the constants that multiply the sum over hydrogen sites $\sum_i$ and the sum over niobium sites $\sum_j$ are approximately equal. Equation (1) becomes

$$\langle \Delta H^2 \rangle = [3.57\times 10^{-46}\textstyle\sum_i (r_i^{-6}) + 3.135\times 10^{-46}\sum_j (r_j^{-6})]\ (\text{Gauss})^2, \quad (2)$$

where r is given in centimeters. Since each hydrogen is likely to have Nb ions as nearest neighbors, the sum $\sum_j$ is considerably larger than the sum $\sum_i$ in Eq. (2). This means that the H-Nb dipole interaction contributes most of the proton NMR second moment.

To apply Eq. (2), it is necessary to specify the interstitial sites in the bcc lattice occupied by hydrogen ions. The order of occupation of octahedral sites previously suggested[13] for NbH_x systems has been used.

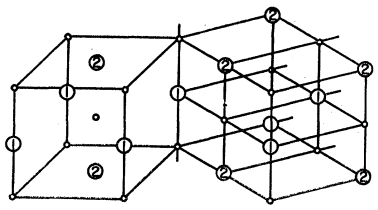

FIG. 1. Assumed interstitial sites of H ions in NbH_x. Small circles represent Nb ions. Numbered sites are H ion sites discussed in Sec. III.

[12] J. Van Vleck, Phys. Rev. 74, 1168 (1948).
[13] T. R. P. Gibb, Jr., *Progress in Inorganic Chemistry* (Interscience Publishers, Inc., New York, 1962), Vol. III.

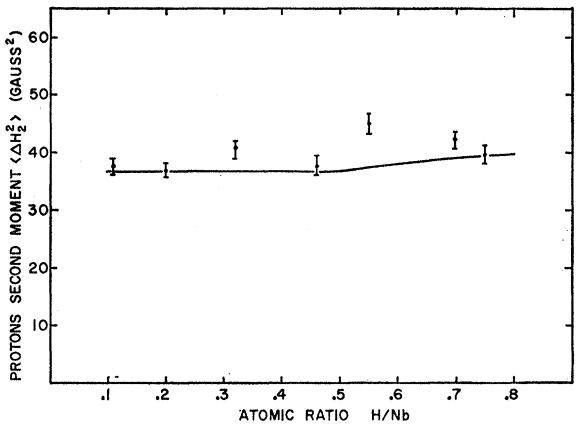

FIG. 2. Concentration dependence of proton second moment in NbH_x at temperature of −197°C. The continuous curve is calculated from Eqs. (2) for $x<0.5$, and from Eqs. (3) and (4) for $x>0.5$. On the scale of this graph, Eqs. (3) and (4) are indistinguishable. Experimental determinations are plotted.

It is assumed that for $0<x<0.5$, NbH_x is a segregated two-phase system of Nb metal and $NbH_{0.5}$ with hydrogen ions occupying the sites (1) in Fig. 1. The lattice constant of this phase $b=3.40$ Å is taken from the article of Trezebiatowski and Stalinski.[2] (For the purposes of this calculation, as well as T_1 and T_2 calculations, it can be assumed that the lattice is cubic.) The contribution from H-H interaction amounts to 1.92 G^2 and the H-Nb contribution is 34.65 G^2. The sum 36.57 G^2 is then plotted as the theoretical second moment between $x=0$ and $x=0.5$ in Fig. 2. After the type (1) sites are full at $x=0.5$, one of two assumptions can be made concerning the occupation of the type (2) sites. These assumptions are (*a*) that sites (2) fill randomly with sites (1) remaining full, or that (*b*) a new two-phase system exists with one phase in which all sites (2) and (1) are full and the other in which only sites (1) are full. Sites (1) form a simple cubic sublattice as do sites (2). Together, sites (1) and (2) have the CsCl structure. The niobium environments around hydrogen sites (1) and (2) are identical, and sites (1) and (2) are equivalent if all hydrogen interstitial sites are full. The lack of equivalence between sites (1) and (2) would occur for $x<1.0$ and any differences would depend only on the order in which sites fill.

Since the Nb environments are equivalent, and since the H-Nb interactions are on the average larger than the H-H interactions, it is not surprising that the second moment according to this model varies little across the concentration range.

For random occupation of sites (2) with sites (1) full [assumption (*a*)], the second moment of hydrides with $x>0.5$ are given by

$$\langle \Delta H^2 \rangle_{(a)} = \langle \Delta H^2 \rangle_{\text{Nb}} + 3.57\times 10^{-46}\times (\text{b}^{-6}) \times [(2x^2-2x+1)(8.40)/x + (2x-1)(20.65)/x]\ (\text{Gauss})^2. \quad (3)$$

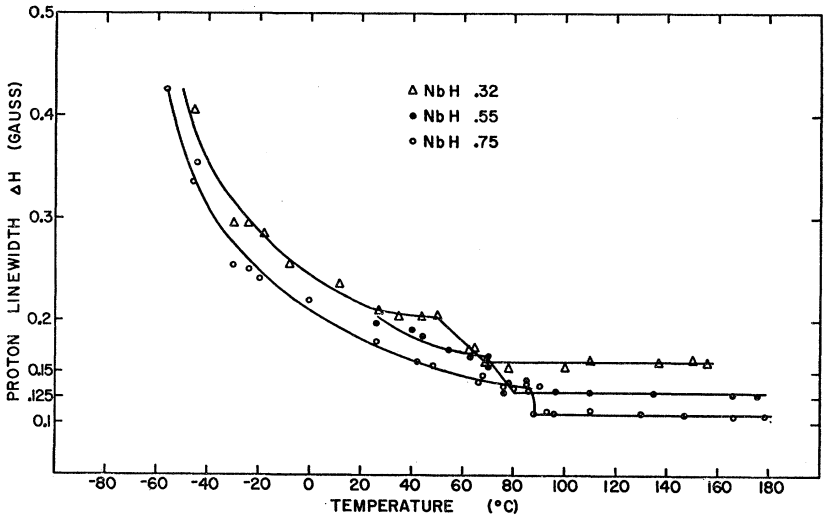

FIG. 3. Temperature dependence of proton linewidth.

In Eq. (3), $\langle\Delta H^2\rangle_{\mathrm{Nb}}$ is the H-Nb contribution, and b is the bcc lattice constant[2] in centimeters. Use of sums[14] of (r^{-6}) for the CsCl structure has been made.

For assumptions (b) above,

$$\langle\Delta H^2\rangle_{(b)}=\langle\Delta H^2\rangle_{\mathrm{Nb}}+3.57\times10^{-46}\times(b^{-6})\times[(2x-1)29.05/x+(1-x)(8.40)/x]\ \ (\mathrm{Gauss})^2. \quad (4)$$

In applying Eqs. (3) and (4), the concentration dependence of the lattice constant b has been included.[2]

Calculations based upon assumptions (a) and (b) are plotted along with experimental determination at 77°K in Fig. 2. The agreement between theory and experiment is fair, but there is little to distinguish assumption (a) from (b). The fact that the measured second moment is concentration independent at $x<0.5$ is evidence of the existence of two phases in this range.

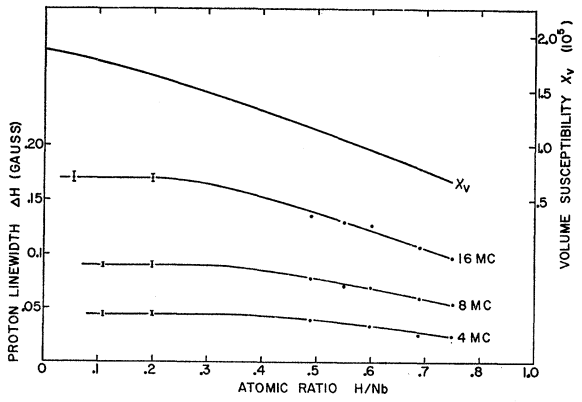

FIG. 4. Concentration dependence of χ_v (from χ_g of Ref. 2) and proton linewidth at the plateau region in different external magnetic fields. The proton Larmor frequency is given in Mc/sec.

2. High-Temperature Linewidths

As the sample temperature is raised, the proton steady-state NMR linewidth decreases. In Fig. 3 temperature dependence of linewidths of three samples are plotted. At temperatures below about −60°C the measurements of width of samples with $x>0.5$ are uncertain because both a wide and a narrow resonance are observed in juxtaposition. This indicates that there are two nonequivalent proton systems in this temperature range. One system is essentially rigid and the other is in a state of motion. Just what distinguishes these two systems is not clear. Similar effects are observed in some compositions of[15] ZrH_x and[8] LaH_x.

At around 100°C, the linewidth ceases narrowing and levels off to a temperature independent "plateau" value that is field dependent. The value of the temperature-independent linewidth is in reasonable agreement with what one would expect from Drain's calculation.[9] A plot of the linewidth plateau ΔH and χ_v versus hydrogen concentration appears in Fig. 4.

Drain estimates that in a close-packed powder sample the broadening due to bulk magnetization of the particles is approximately $3\chi_v H_0$, where χ_v is the volume magnetic susceptibility and H_0 is the external field. The volume susceptibility[2] of NbH_{x0} ranges from 19×10^{-6} to 6×10^{-6} as x ranges from 0–0.8. In a resonant field of 3760 G (proton Larmor frequency=16 Mc/sec), the bulk magnetization broadening would be about 0.08 G for $NbH_{0.7}$. The broadening depends on particle shape as well as packing of particles and the estimate here should be considered as approximate. External field inhomogeneity across the sample is $\leq$0.02 G at 3760 G.

Several experimental checks can be made on this mechanism: (a) the value of the linewidth plateau should be field-dependent, (b) the plateau height should

[14] H. S. Gutowsky and B. R. McGarvey, J. Chem. Phys. **20**, 1472 (1952).

[15] J. F. Hon, J. Chem. Phys. **36**, 739 (1962).

demonstrate the same x dependence that χ_v has, and (*c*) since this broadening is inhomogeneous,[16] the value of T_2 determined by spin-echo experiments should continue to increase due to diffusion of hydrogen ions while the linewidth ΔH stays constant in the plateau region. Plots of measured absorption peak-peak linewidth, ΔH versus external field in Fig. 6 and ΔH versus χ_v in Fig. 5 show the linear dependence on H_0 and χ_v as indicated in (*a*) and (*b*) above. The linearity of the ΔH versus χ_v curve is better than expected since it is compiled from several samples with varying particle size and packing. The external field inhomogeneity appears as the ΔH axis intercept. χ_v was calculated from χ_g (mass susceptibility) using the appropriate density for each hydrogen concentration. ΔH in Fig. 5 was measured at $\sim$100°C while χ_g (and hence χ_v) was measured at room temperature.[2] The correction is small due to the small temperature dependence of χ_g. In addition, we have to correct for the fact that at room temperature the low concentration samples ($x<0.5$) contain two phases. The values of χ_v for these phases are likely to be different. Since we do not know these values of χ_v, we cannot make the correction. This could be the reason for the fact that the low concentration samples deviate from the straight line in Fig. 5.

A plot of spin-echo measurements of $(1/T_2)$ the spin-echo decay rate, in Fig. 7, indicates that $(1/T_2)$ continues to decrease at temperatures above room temperature. The fact that numerical values of $(1/T_2)$ in the plateau region are about one-tenth the half-width of the steady-state resonance expressed in similar units is consistent with the experimental check (*c*) proposed above. For $NbH_{0.7}$, half-width of the absorption expressed in angular frequency units is about 1×10^3 sec^{-1}.

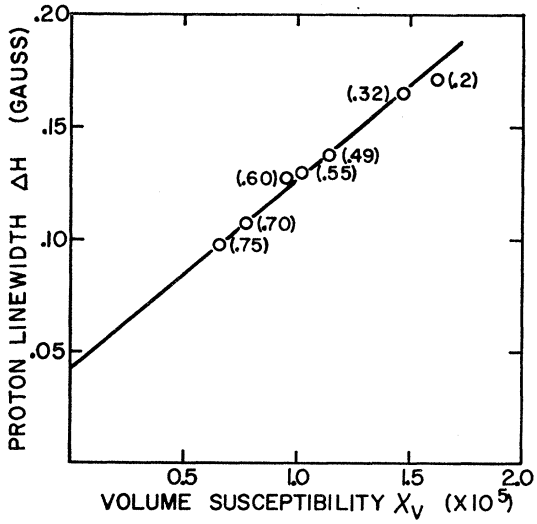

FIG. 5. Proton linewidth at the plateau region versus χ_v for different samples. H/Nb ratio is given in parenthesis.

[16] A. Abragam, *Principles of Nuclear Magnetism* (Oxford University Press, New York, 1961).

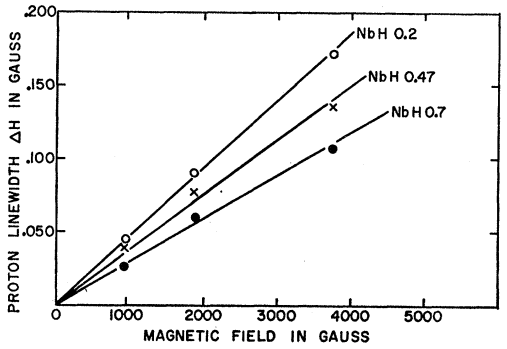

FIG. 6. Magnetic field dependence of proton linewidth at the plateau region.

At temperatures *above* the onset of the plateau, $(1/T_2)$ experiences a minimum and then increases as temperature increases. The high-temperature increase in spin-echo decay rate is caused by hydrogen ion diffusion in magnetic field gradients within each particle. It will be shown in Sec. III3 that the actual jump frequency of protons at the temperature of the minimum in $(1/T_2)$ is about $(\tau^{-1})=2\times10^{10}$ per second. At this jump frequency a proton can move a distance $L\approx(t/\tau)^{1/2}l$ in t seconds using steps of length l. Using $t=T_2=10^{-2}$ sec, $l=2.3\times10^{-8}$ cm, $L\approx3\mu$, which is an appreciable fraction of the particle size used in these experiments. Proton diffusion in the demagnetization

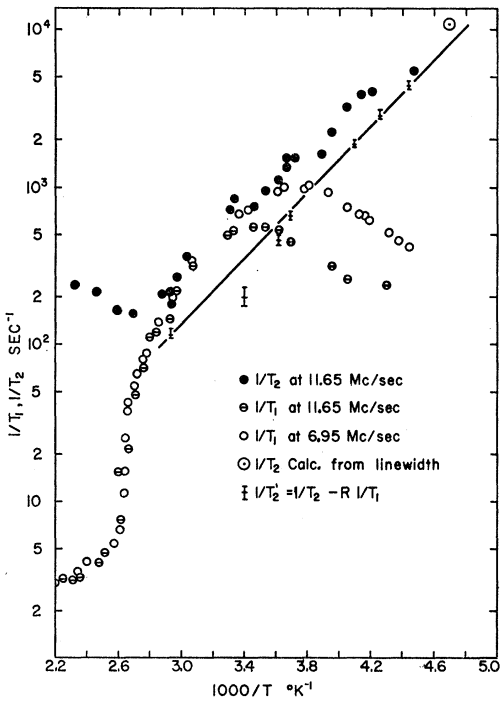

FIG. 7. $1/T_1$, $1/T_2$ and $1/T_2'$ versus temperature for protons in $NbH_{0.7}$.

field gradient within a particle due to its own irregular shape is probably more effective in increasing the spin-echo decay rate than is diffusion in field gradients due to neighboring polarized particles. Some preliminary Carr-Purcell[11] pulse-train experiments yield lower value of $(1/T_2)$ than those obtained by a spin-echo experiment. It can be concluded that the increase in $(1/T_2)$ at high temperatures is caused by diffusion in field gradients within each particle.

It will be noted in Fig. 3 that just at the low-temperature side of the plateau that there is a fairly steep drop in the linewidth of about 20–40 mG. This drop is believed to be due to an increased rate of diffusion at the onset of the plateau. Changes in diffusion in this temperature region are discussed in more detail in Sec. III4.

The absorption curves of NbH_x, $x \gtrsim 0.4$ are asymmetric at temperatures below the steep drop in linewidth and become symmetric at high temperatures. When the line is symmetric, its shape is definitely *not* Lorentzian as might be expected for motionally narrowed lines. The symmetric resonances have steeper wings than in a Lorentzian and the observed shape must be representative of the field distribution within the particles.

The measurements of the spin-echo dephasing time T_2 and the thermal relaxation time T_1 as a function of temperature are used to determine the temperature dependence of τ. An approximation is made for translational diffusion which neglects correlation effects on jump sequences and assumes the spectral density (assumed form of the correlation function $\exp[-t/\tau)]$, of the dipolar interaction depends on ω and τ as

$$J(\omega) \propto 2\tau/(1+\omega^2\tau^2).$$

The average time between jumps is τ. By combining the contributions from like and unlike spins, T_2 is expressed by[16]

$$\frac{1}{T_2} = C_I\{(15/4)J^{(1)}(\omega_I)+\tfrac{3}{8}J^{(2)}(2\omega_I)+\tfrac{3}{8}J^{(0)}(0)\} + C_S\{\tfrac{1}{6}J^{(0)}(0)+(1/24)J^{(0)}(\omega_I-\omega_S)+\tfrac{3}{4}J^{(1)}(\omega_I) + \tfrac{3}{2}J^{(1)}(\omega_S)+\tfrac{3}{8}J^{(2)}(\omega_I+\omega_S)\}, \quad (5)$$

and T_1 is given by Eq. (12) in Sec. III3 below.

In Eq. (5), $C_I=\gamma_I{}^4\hbar^2 I(I+1)$, $C_S=\gamma_I{}^2\gamma_S{}^2\hbar^2 S(S+1)$, $\omega_I=\gamma_I H_0$, and $\omega_S=\gamma_S H_0$. The ratio of C_S to C_I is $C_S/C_I=1.98$. Assuming cubic symmetry, the average over the directional dependence of the spectral density functions for dipolar coupling[16] can be expressed in the usual form in terms of $J^1(\omega)$ so that

$$J^2(\omega):J^1(\omega):J^0(\omega)=4:1:6 \quad (6)$$

and

$$J^{(1)}(\omega)=\frac{2}{15}\left(\frac{2\tau}{1+\omega^2\tau^2}\right)\sum_k(r_k{}^{-6}). \quad (7)$$

In Eq. (7), $\sum_k(r_k{}^{-6})$ is summed over like (I) sites and unlike (S) sites for the $J(\omega)$ that appear with C_I and C_S, respectively. The values of these sums obtained from the second-moment calculation are used. The contributions to $1/T_2$ from the secular broadening are given by the terms containing $J^0(0)$. Calling these terms $1/T_2'$,

$$1/T_2' = \tfrac{3}{5}C_I\tau\textstyle\sum_i(r_i{}^{-6})+(4/15)C_S\tau\sum_j(r_j{}^{-6})$$
$$1/T_2' = \gamma_I{}^2\langle\Delta H^2\rangle\tau. \quad (8)$$

Equation (8) is equivalent to the expression for $1/T_2$ derived by Kubo and Tomita,[17]

$$\left(\frac{1}{T_2}\right)^2=\frac{4\ln 2}{\pi}\langle\Delta\omega^2\rangle\arctan\left[\frac{\pi\tau}{(4\ln 2)T_2}\right], \quad (9)$$

where $\langle\Delta\omega^2\rangle=\gamma_I{}^2\langle\Delta H^2\rangle$ and it is assumed $\langle\Delta\omega^2\rangle^{1/2}\tau\ll 1$, so that $\tau\ll T_2$. One must also assume $\omega_I\tau\gg 1$ so that contributions from T_1 to the observed $1/T_2$ are negligible.

At high temperatures where $\omega_I\tau\ll 1$, the expressions for T_1 and T_2 become equal and

$$\frac{1}{T_1}=\frac{1}{T_2}=2C_I\tau\textstyle\sum_i(r_i{}^{-6})+\frac{4}{5}C_S\tau\sum_j(r_j{}^{-6}). \quad (10)$$

Equation (10) can be used to find the correction to be used on experimental data for T_2 to obtain T_2' in this temperature region where T_2 is principally determined by T_1

$$(1/T_2')=(1/T_2)-R(1/T_1).$$

The constant R is given by

$$R=1-\left[\frac{(9/4)C_I\sum_i(r_i{}^{-6})+C_S\sum_j(r_j{}^{-6})}{15/2C_I\sum_i(r_i{}^{-6})+5C_S\sum_j(r_j{}^{-6})}\right]. \quad (11)$$

In the intermediate region $\omega_I\tau\approx 1$, the value of $R=(1/T_2-1/T_2')/(1/T_1)$ could be estimated for any value of of τ. The accuracy of such an estimate of R may be questionable because of the model of the correlation function used in the derivation.

However in the limit $\omega\tau\ll 1$, $J^{(q)}(\omega)$ will be proportional to τ for any reasonably well-behaved correlation function.[18] Then the relative values of $J^{(q)}(\omega)$ are determined by Eq. (6) and the above estimate of R should be valid. Also, at high temperatures, $\omega_I\tau\ll 1$, and $1/T_1$ is proportional to τ. The temperature dependence of T_1 will clearly reflect the temperature dependence of τ.

It was found that the proton absorption resonances are shifted relative to water to a higher field (diamagnetic). The shift is linear with applied field, and it is, within measurement error, independent of concentration with the exception of $NbH_{0.05}$ where no shift is observed. The measured value of the shift is $|\Delta H/H| = 1.6\times 10^{-3}\%$.

3. Thermal Relaxation Times

Figures 7 and 8 show plots of proton thermal relaxation times T_1, as a function of $(1/T)$. Measurements of

[17] R. Kubo and K. Tomita, J. Phys. Soc. Japan **9**, 888 (1954).
[18] C. P. Slichter, *Principles of Magnetic Resonance* (Harper and Row, New York, 1963).

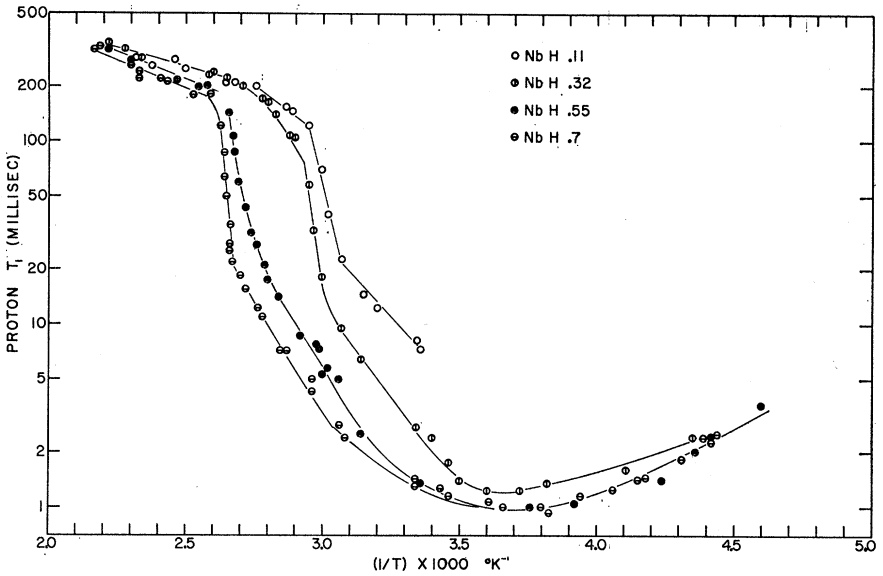

FIG. 8. Temperature dependence of thermal relaxation time T_1 for protons in NbH_x at 6.95 Mc/sec.

T_1 were made by both 90–90° and 180–90° pulse sequences at frequencies of 6.95 and 11.65 Mc/sec.

Proton spin-lattice relaxation is caused by a modulation of H-H and H-Nb magnetic dipole interactions due to translational diffusion. The minimum of T_1 at temperatures near -10 to -30°C indicates that the jump frequency τ is approximately equal to the Larmor angular frequency at these temperatures. A sharp rise in T_1 at temperatures above room temperature is evident. The temperature T_p of the rise is concentration-dependent and is due to a sharp decrease in τ.

To obtain temperature dependence of τ, the T_1 data are compared to theory[16] for relaxation of spin system I, interacting with itself and a second system S. The expression for T_1 for protons (system I) is

$$1/T_1=\tfrac{3}{2}C_I\{J^{(1)}(\omega_I)+J^{(2)}(2\omega_S)\}+C_S\{\tfrac{1}{12}J_{IS}{}^{(0)}(\omega_I-\omega_S)+\tfrac{3}{2}J_{IS}{}^{(1)}(\omega_I)+\tfrac{3}{4}J_{IS}{}^{(2)}(\omega_I+\omega_S)\}. \quad (12)$$

By using Eq. (6) and $C_S=1.98C_I$,

$$1/T_1=(\tfrac{3}{2})C_I\{J^{(1)}(\omega_I)+4J^{(1)}(2\omega_I)+0.66J_{IS}{}^{(1)}(0.76\omega_I)+1.98J_{IS}{}^{(1)}(\omega_I)+3.96J_{IS}{}^{(1)}(1.24\omega_I)\}. \quad (13)$$

From the assumed form of $J^{(q)}(\omega)$, Eq. (13) becomes

$$(1/T_1)=\tfrac{2}{5}C_I\left[\left(\frac{1}{1+(\omega_I\tau)^2}+\frac{4}{1+(2\omega_I\tau)^2}\right)\tau\sum_i(r_i^{-6})+\left(\frac{0.66}{1+(0.76\omega_I\tau)^2}+\frac{1.98}{1+(\omega_I\tau)^2}+\frac{3.96}{1+(1.24\omega_I\tau)^2}\right)\tau\sum_j(r_j^{-6})\right]. \quad (14)$$

The maximum value of $(1/T_1)$ for protons occurs near $\omega_I\tau=1$ at a value which depends on the relative values of $\sum_i(r_i^{-6})$ for H sites and $\sum_j(r_j^{-6})$ for Nb sites.

For the assumed occupation of interstitial sites (1) and (2), $\sum_j(r_j^{-6})=173(b^{-6})$ for H-Nb and $\sum_i(r_i^{-6})$ varies between $8.4(b^{-6})$ at $NbH_{0.5}$ to $29(b^{-6})$ at $NbH_{1.0}$ where b is the edge of the (approximate) bcc unit cell. It then follows that H-Nb dipole interactions dominate the relaxation mechanism and that as H concentration increases, the value of T_1 minimum should decrease slightly.

A calculation of the minimum value of T_1 in $HbH_{0.7}$ based on Eq. (14) is $T_1=0.76$ msec at 6.95 Mc/sec compared to a measured value of 1.0 msec.

4. Diffusion

From inspection of the curves of T_1 versus $1/T$ in Fig. 8, one sees that there are several features that the samples have in common. The shapes of the curves are similar for all samples and the temperatures of the T_1 minimum vary between -15 to $+10$°C. Therefore the values of ν_0, the frequency factor, and E_a, the activation energy, do not vary greatly over the concentration range observed. There is a sharp rise in T_1 in the high-temperature region which is more distinct in the high-concentration samples. Since $(1/T_1)\propto\tau$ in this temperature range, the sharp rise in T_1 corresponds to a sharp decrease in τ. We think that this change in τ is coupled with a phase transition in the NbH_x systems and will refer to the temperature at the point about halfway up the "step" in T_1 as the transition temperature T_p. The evidence for the phase transition is discussed in Sec. V in more detail.

A check for consistency in the theory for $(1/T_1)$ and $(1/T_2)$ versus τ is made for the sample $NbH_{0.7}$ for which there is T_1 data at two Larmor frequencies, $(\omega_I/2\pi)=6.95$ and 11.65 Mc/sec and T_2 data at 11.65 Mc/sec.

For $NbH_{0.7}$ the ratio of the sums $[\sum_i(r_i^{-6})/\sum_j(r_j^{-6})]$ is 0.11 and $\sum_j(r_j^{-6})=173(b^{-6})$ where b is the lattice constant of the (distorted) bcc lattice.

On the high-temperature side of the T_1 minimum ($1/T_1$ maximum) there is a small temperature range near $1/T=2.8\times10^{-3}$ ($°K^{-1}$) where it can be assumed $\omega\tau$ is small and where effects of diffusion in the demagnetization fields are negligible. The T_1 correction to the measured T_2 is made by first calculating R in Eq. (11). For $NbH_{0.7}$, one finds $R=0.88$. Then,

$$(1/T_2')=(1/T_2)-0.88(1/T_1).$$

At large values of $\omega\tau$, low temperature, it is found that for $\omega\tau\geq10$, $(1/T_2-1/T_2')\approx6(1/T_1)$. The large number 6 is mainly due to the large contribution of the $J^{(1)}(\omega_S)$ term in Eq. (5). The temperature dependence of T_2' is estimated by the equation,

$$(1/T_2')=(1/T_2)_{\text{meas}}-R(1/T_1)_{\text{meas}},$$

where $R=0.88$ at high temperatures and $R\approx6$ at low temperatures. R varies as a smooth function of $(1/T)$ between the above limits in the intermediate temperature range. The measured values of $(1/T_2)$ are thus corrected to determine $(1/T_2')$ which is plotted versus $(1/T)$ in Fig. 7. In the region of the maximum of $(1/T_1)$ the value of R appears to be too large and overcorrection is evident. The limiting values of R, 0.88, and 6, are the most reliable and occur where the T_1 correction is small anyway. These values of T_2' are given emphasis in drawing in a straight line to represent $(1/T_2')$ versus $(1/T)$. Now, since $(1/T_2')=\langle\Delta\omega^2\rangle\tau=\langle\Delta\omega^2\rangle(\nu_0^{-1})\exp(E_a/RT)$, a fit to $\ln(1/T_2')$ versus $(1/T)$ can be made by using $\nu_0=3.1\times10^{11}(\text{sec}^{-1})$ and $E_a=4.9\pm0.3$ kcal/mole.

Another approach to the temperature dependence of τ is obtained by comparing the measured dependence of $(1/T_1)$ on temperature and the theoretical dependence of $(1/T_1)$ on τ in Eq. (14). In making the comparison relative values of T_1, in the form $(T_1/T_{1\min})$, are used. The resulting values of τ are plotted as full circles and open circles for 6.95- and 11.65-Mc/sec data, respectively, on Fig. 9. The sharp drop in τ is evident near 100°C. Agreement between values of τ obtained from data for two Larmor frequencies is fair.

From the slopes of the continuous line drawn through the data points,

for $3.0(°K^{-1})<10^3/T<4.5(°K^{-1})$,

$$E_a=5.0\pm0.3 \text{ kcal/mole}$$
$$\nu_0=5\times10^{11}(\text{sec}^{-1})$$

and for $10^3/T<2.6(°K^{-1})$,

$$E_a=3.7\pm0.3 \text{ kcal/mole}$$
$$\nu_0=1.9\times10^{12}(\text{sec}^{-1}).$$

There is good agreement within experimental uncertainties between values of E_a and ν_0 obtained from T_2 and T_1 measurements in the low-temperature phase. The increased diffusion rate of H ions above T_p is due both to a decrease in E_a and an increase in ν_0, the frequency factor. These changes in E_a and ν_0 are about equally effective in decreasing τ in the high-temperature phase.

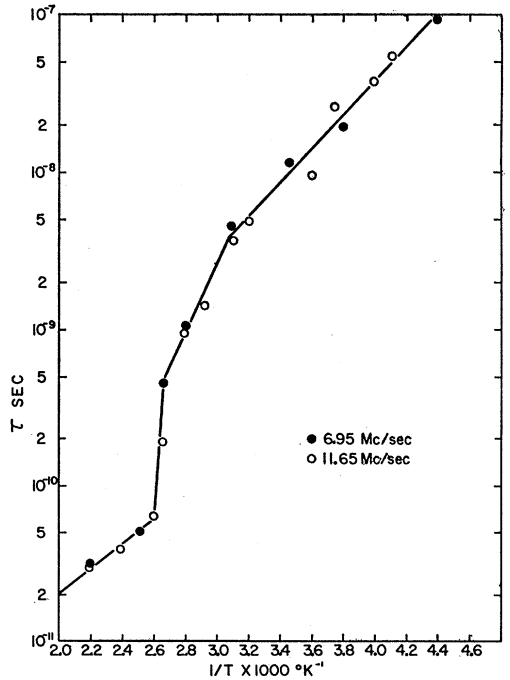

FIG. 9. Temperature dependence of correlation time τ for protons in $NbH_{0.7}$ calculated from T_1.

IV. NIOBIUM MAGNETIC RESONANCE

1. Linewidth and Intensity

The width and intensity of the niobium magnetic resonance absorption are affected by quadrupole interactions at low temperatures in all hydrogen concentrations. In the low-temperature region $T<T_p$, the observed signal decreases as x in NbH_x increases. For values $x>0.5$ the low-temperature resonance is very weak or unobservable.

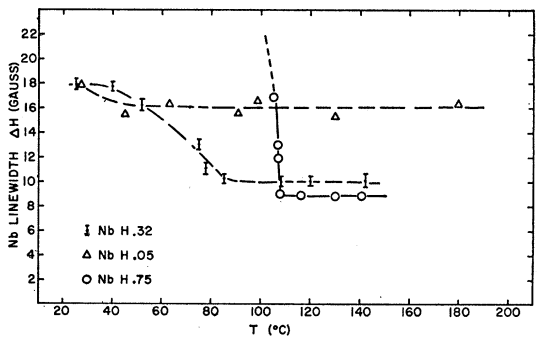

FIG. 10. Temperature dependence of Nb linewidth in NbH_x.

In the low concentration $x \leq 0.1$ samples, there is little change in linewidth with temperature. At intermediate concentrations, $0.1 < x < 0.5$, the linewidth narrows appreciably at high temperature. At the high concentrations, the resonance is not well observed unless $T > T_p$, and then the narrowing and increase in observed intensity is sharp. Typical linewidth behavior is plotted in Fig. 10. At high temperatures the Nb-Nb dipole interaction is estimated to contribute 7.1 G to the linewidth.

A striking feature of the high-temperature Nb data is that the intensity increases upon narrowing. In the high-concentration hydrides with $x \geq 0.5$, the observed fraction of the maximum possible Nb resonant intensity is actually larger than in the Nb parent metal. That there is an intensity reduction below maximum means that not all possible $\Delta m = 1$ transitions in the niobium energy level scheme are observed. The nuclear electric quadrupole interaction shifts all ten of the Nb energy levels ($S = \frac{9}{2}$) so that most of the transition frequencies do not equal the Larmor frequency. If the average electric field gradient experienced by Nb nuclei produces full first-order broadening, but is too small for second-order effects,[6] then the observed Nb resonance will be due to $m = \frac{1}{2}$ to $m = -\frac{1}{2}$ transitions only. This transition has an intensity of 15.1% of the intensity associated with all $\Delta m = 1$ transitions.

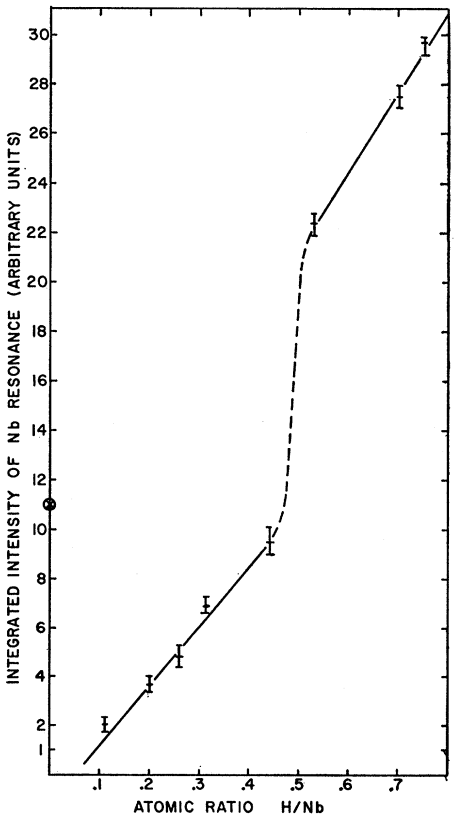

FIG. 11. Integrated intensity of Nb in NbH_x at 150°C. The point on the vertical axis represents Nb metal at 150°C.

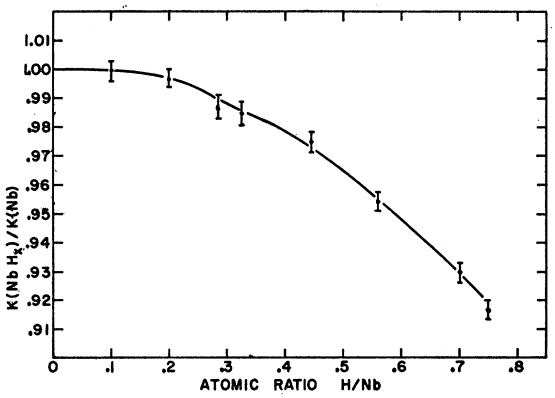

FIG. 12. Ratio of Knight shift of Nb^{93} in NbH_x to Knight shift in Nb metal at 150°C.

In the Nb metal (99.7 wt% pure) used for sample preparation, 11% of maximum intensity is observed. The metal was purchased in the form of 325 mesh powder. Since fewer than all $m = \frac{1}{2} \leftrightarrow m = -\frac{1}{2}$ transitions are observed, one can conclude that the powder particles are cold-worked. Signal intensity as determined experimentally by comparison with a known amount of 99.99% pure aluminum in which all $\Delta m = 1$ transitions are observed.

The fact that high-temperature Nb resonance intensity per Nb atom in the hydride is greater than 15% and that it is stronger than in the solvent metal indicates that there is a much smaller average electric field gradient at Nb nuclei in the hydride than in the metal. This intensity dependence indicates that the high-temperature phase $T > T_p$ is cubic. A plot of relative niobium intensity for various hydrogen concentrations at $T > T_p (T = 150°C)$ is shown in Fig. 11. The growth in intensity with x implies that the hydrogen rich $x \geq 0.5$ phase is the main contributor to the observed resonance at $T > T_p$. The concentration dependence of Nb absorption intensity in the low-temperature phase $T < T_p$ indicates that only the hydrogen poor $x < 0.1$ phase is observed.

2. Nb Knight Shift

The niobium Knight shift K was measured at 150°C in the same structural phase for all hydrogen concentrations. Figure 12 shows that the value of K decreases by 9% at $NbH_{0.75}$ while the susceptibility has decreased by almost 60%.

If the hydrogen exists as a positive ion,[19] then the hydrogen would contribute some electron density to the conduction band. It is known that when the electron per atom ratio in Nb is increased by substitutional

[19] C. K. Coogan and H. S. Gutowsky, J. Chem. Phys. **36**, 110 (1962).

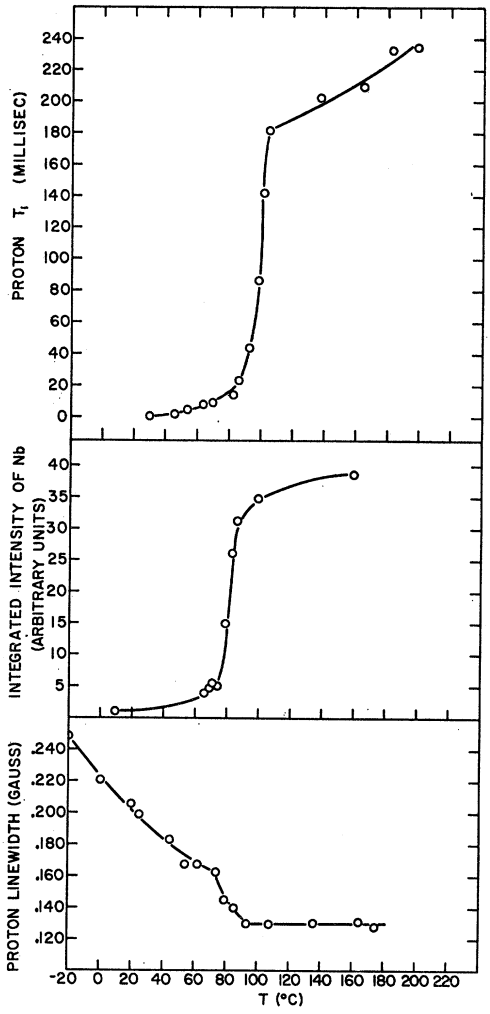

FIG. 13. Transition temperature T_p in $NbH_{0.55}$ from: (a) T_1 of protons; (b) integrated intensity of Nb; (c) protons linewidth.

alloying[20,21] the density of states at the Fermi surface is decreased, susceptibility is decreased and the Nb Knight shift is decreased. Assuming that addition of hydrogen adds electrons to the Nb conduction band and increases the electron per atom ratio, then the change in K with concentration is in the same direction as the Nb alloys. However, the situation is certainly not that simple, for the value of K for Nb is determined by contributions from s-band paramagnetism, d-band paramagnetism through s-core polarization, and second-order orbital paramagnetism.[22]

It should be noted that the Knight shift of V in $VH_{0.66}$ is increased over that in pure vanadium metal.[23] In vanadium, a decrease in core polarization would make its contribution to K_V less negative. If the s band and orbital susceptibility contributions to K_V are decreased by H addition, then the decrease in core polarization must be large enough to more than compensate for their decrease and K_V increases. Competition between change of a negative core polarization and positive s band and orbital contributions to K in niobium may account for the small change in K that is observed. The only other known measurements of K of the solvent atom nucleus in transition metal hydrides, that of La in LaH_x, demonstrate large fractional decreases of K and suceptibility.[8]

V. PHASE TRANSITION, CONCLUSIONS

From the above discussed measurements on proton linewidth T_1 and T_2, it is evident that there is a distinct change in the diffusion of hydrogen in the NbH_x system in the region between 60–100°C. As temperature is increased, the characteristic jump time τ decreases markedly over a small range of temperatures determined by the hydrogen concentration. The temperature at the center of the range is termed T_p. The change in τ is more distinct at higher concentrations but it is never so sharp as to be termed a discontinuity.

The niobium linewidth and intensity measurements indicate that the above described temperature dependence of τ is due to a phase transition in NbH_x. It is known from x-ray studies[3,5] that the low-temperature hydrogen-rich phase is orthorhombic (slightly distorted bcc) and that the high-temperature phase is cubic. The x-ray data do not clearly identify the phase transition temperature. The niobium resonance linewidth results mainly from Nb-Nb and Nb-H dipolar coupling and from Nb quadrupole interactions due to a Nb environment of low symmetry. The Nb-H dipole interaction will be motionally averaged to zero in the same temperature range as the protons, which is well below T_p. The quadrupole interaction, which can reasonably be expected to be 10^6 (sec^{-1}) or more, could be due to a nonsymmetric hydrogen environment around the Nb nucleus or a noncubic Nb lattice or both. The quadrupolar contributions from the hydrogen ions will

TABLE I. This table is a comparison of transition temperature in NbH_x determined in three different ways: a, from temperature dependence of proton linewidth (see Fig. 3); b, from temperature dependence of proton T_1; c, from temperature dependence of Nb linewidth (see Fig. 10).

Sample H/Nb	a	b	c
0.11		58°C	
0.20	55°C		60°C
0.32	60°C	64°C	65°C
0.47		68°C	68°C
0.55	80°C	97°C	85°C
0.70	95°C	104°C	92°C
0.75	86°C	80°C	105°C

[20] D. W. Jones and A. D. McQuillan, Phys. Chem. Solids **23**, 1441 (1962).
[21] S. Alexander, E. Corenzwit, B. T. Matthias, R. G. Shulman, and B. J. Wyluda, Phys. Rev. **129**, 2481 (1963).
[22] A. M. Clogston, A. C. Gossard, V. Jaccarino, and Y. Yafet, Phys. Rev. Letters **9**, 262 (1962).
[23] R. Oriani, E. McCliment, and J. F. Youngblood, J. Chem. Phys. **27**, 330 (1957).

will be effectively averaged out when $\omega_Q\tau \ll 1$, where ω_Q is a measure of the quadrupole interaction strength. Even if the hydrogen ion contribution is averaged out, a noncubic Nb environment will still broaden and weaken the observed resonance.

A transition from orthorhombic to cubic structure would greatly reduce Nb electric quadrupole interaction, and this would be observed as a Nb line narrowing and intensity growth. These changes in the Nb resonance do indeed occur and they coincide with the steep change in τ at $T \approx T_p$. It then seems reasonable that the change in τ is closely associated with a phase transition from the orthorhombic phase to the cubic phase.

The observed resonance changes at T_p are not sharp enough to define T_p unambiguously. Compare in Fig. 13, the proton T_1, proton linewidth ΔH, and the Nb intensity for $NbH_{0.55}$ versus temperature. The data suggest that the change occurs over a range starting from about 80°C and extending to 98–100°C. The gradual nature of this transition suggests that the transition is a second-order transition.

In Table I, the transition temperature range as determined by three measurements is given for several hydrogen concentrations. These data are plotted in Fig. 14 along with the transition temperatures calculated by Albrecht, Goode, and Mallett.[3] To the authors' knowledge there are no other known measurements to further establish the nature of this transition.

The linewidth and T_2 data for protons demonstrate the existence of magnetic field gradients within sample particles due to bulk paramagnetism. These magnetic field gradients produce the minimum NMR linewidth plateau at high temperatures. Measurements of spin-echo decay time confirm inhomogeneous broadening of the steady-state linewidths and also demonstrate effects of translational diffusion through these field gradients. These effects are more pronounced in a sample of small particles, as used in NMR in metals, than in a large single unit sample. Therefore the effects of diffusion within these gradients can be observable because of the relatively high gradients encountered and the small particle size over which diffusion will occur. The high-temperature plateau might easily be unobservable or mistaken as an inhomogeneity of external field in materials of low susceptibility.

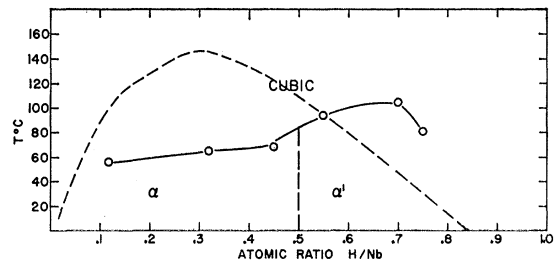

FIG. 14. Phase diagram of NbH_x system. Full line: from data on T_1 of protons; broken line: from Ref. 3.

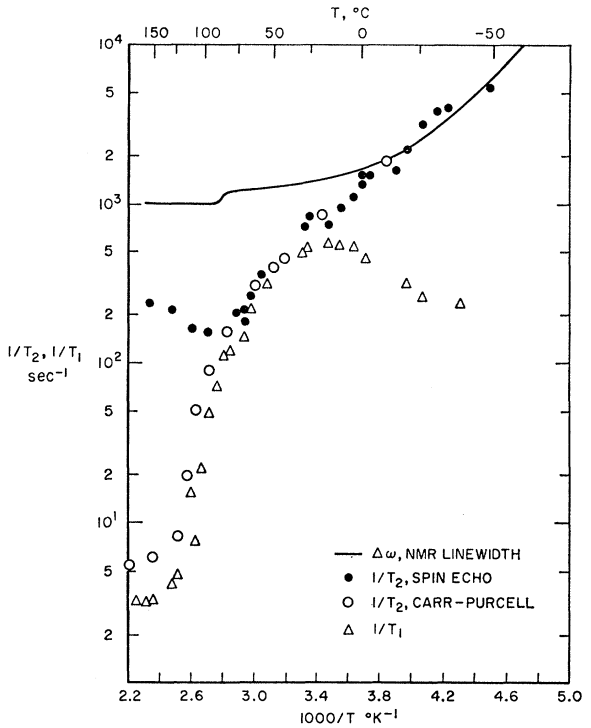

FIG. 15. Measurements of NMR linewidth in radians/second, $(1/T_2)$ determined by the two-pulse spin-echo method, $(1/T_2)$ determined by Carr-Purcell method, and $(1/T_1)$ at 11.65 Mc/sec in $NbH_{0.7}$. The difference between $\Delta\omega$ and $(1/T_2)$, spin echo, demonstrates inhomogeneous broadening due to the powder sample demagnetization field. The differences between $(1/T_2)$, spin echo, and $(1/T_2)$, Carr-Purcell, show the effects of self-diffusion of protons in the demagnetization field gradients.

ACKNOWLEDGMENTS

We thank David Rohy for preparation of samples and assistance with taking data and its analysis. R. C. Wayne assisted in data taking. Early in this work, several conversations with Dr. D. S. Schreiber were valuable.

[*Note added in proof.* We have recently measured $(1/T_2)$ in $NbH_{0.7}$ using the Carr-Purcell technique at 11.65 Mc/sec. The results are shown in Fig. 15. In the limiting case of short spacing between the 180° pulses in the Carr-Purcell train, the effects of diffusion in the determination of $(1/T_2)$ are negligible. Under these circumstances the agreement between $(1/T_2)$ and $(1/T_1)$ is substantially improved in the high-temperature (greater than 90°C) region. The difference between values of $(1/T_2)$ determined by a two-pulse spin-echo technique (Fig. 7) and the values of $(1/T_2)$ determined by the Carr-Purcell technique (Fig. 15) demonstrates that the effects of diffusion in the demagnetization field gradient can be important in the study of a motionally narrowed NMR line.]